

# FIRST-ORDER SYSTEM LEAST-SQUARES FOR THE OSEEN EQUATIONS

SANG DONG KIM\*, CHANG-OCK LEE†, THOMAS A. MANTEUFFEL‡, STEPHEN F. MCCORMICK§,  
AND OLIVER RÖHRLE¶

**Abstract.** Following earlier work for Stokes equations, a least-squares functional is developed for two- and three-dimensional Oseen equations. By introducing a *velocity flux* variable and associated curl and trace equations, ellipticity is established in an appropriate product norm. The form of Oseen equations examined here is obtained by linearizing the incompressible Navier-Stokes equations. An algorithm is presented for approximately solving steady state, incompressible Navier-Stokes equations with a Nested Iteration-Newton-FOSLS-AMG iterative scheme, which involves solving a sequence of Oseen equations. Some numerical results for Kovasznay flow are provided.

**Key words.** least-squares discretization, Oseen equations, nested iteration

**AMS(MOS) subject classifications.** 65F10, 65F30

**1. Introduction.** Over the last decade, many successful theories were developed for a first-order system formulation of Stokes and Navier-Stokes equations (see [1, 2, 3, 4, 5, 6, 7]). The first-order system introduced in [7] for Stokes equations involved *velocity*,  $\mathbf{u}$ , a new dependent variable,  $\mathbf{U} = \nabla \mathbf{u}^t$ , refer to as *velocity flux*, and *pressure*,  $p$ . The least-squares functional using  $L^2$  and  $H^{-1}$  norms weighted appropriately by the viscosity constant,  $\mu$ , was shown to be elliptic in the sense that its homogeneous form is equivalent to squared product norm  $\mu^2 \|\mathbf{U}\|^2 + \mu^2 \|\mathbf{u}\|_1^2 + \|p\|^2$ . Furthermore, with the extended first-order system, which includes equations involving *trace* and *curl* related to *velocity flux*, it was shown that the functionals using an  $L^2$  norm weighted by  $\mu$  is elliptic in the sense of squared product norm  $\mu^2 \|\mathbf{U}\|_1^2 + \mu^2 \|\mathbf{u}\|_1^2 + \|p\|_1^2$  (see [7]). This equivalence of the first-order system least-squares method enables us to use standard finite element spaces to discretize the equations and multigrid methods to solve the resulting linear systems with respective optimal approximation and solver properties (see, for example, [8]).

The purpose of this paper is to apply this methodology to the steady-state, incompressible Navier-Stokes equations with a linearized convection term, which yields the Oseen equations. A method for linearization of the Navier-Stokes equations is to introduce a known function,  $\beta$ , considered as an approximation of velocity,  $\mathbf{u}$ , in the convection terms. Thus,  $(\nabla \mathbf{u}^t)^t \mathbf{u}$  is replaced by  $(\nabla(\mathbf{u}^t + \beta^t))^t(\mathbf{u} + \beta)$ , which is linearized as  $(\nabla \mathbf{u}^t)^t \beta + (\nabla \beta^t)^t \mathbf{u} + (\nabla \beta^t)^t \beta$ . As in [7], we begin by reformulating the Oseen equations in two or three dimensions as a first-order system in terms of a *velocity flux* variable, and then apply least-squares principles to this system using  $L^2$  and  $H^{-1}$  norms, which produces a functional we call  $G_1$  (see (3.1)). This system can be further extended to a first-order system with equations involving the curl and grad trace of the velocity flux variable. The associated least-squares functional, formed by summing  $L^2$  norms of each equation, we call  $G_2$

---

\*Department of Mathematics Education, Kyungpook National University, Taegu, Korea 702-701 (skim@sobolev.knu.ac.kr). This work was sponsored by the Korea Research Foundation under grant KRF-2002-070-C00014.

†Division of Applied Mathematics, KAIST, Daejeon, 305-701, Korea (colee@amath.kaist.ac.kr). This work was sponsored by KOSEF R01-2000-00008.

‡Department of Applied Mathematics, Campus Box 526, University of Colorado at Boulder, Boulder, CO 80309-0526 (tmanteuf@colorado.edu). This work was sponsored by the Department of Energy under grant numbers DE-FC02-01ER25479 and DE-FG02-03ER25574, Lawrence Livermore National Laboratory under contract number B541045, Sandia National Laboratory under contract number 15268, and the National Science Foundation under grant numbers DMS-0410318.

§Department of Applied Mathematics, Campus Box 526, University of Colorado at Boulder, Boulder, CO 80309-0526 (stevem@colorado.edu). This work was sponsored by the Department of Energy under grant numbers DE-FC02-01ER25479 and DE-FG02-03ER25574, Lawrence Livermore National Laboratory under contract number B541045, Sandia National Laboratory under contract number 15268, and the National Science Foundation under grant numbers DMS-0410318.

¶Bioengineering Institute, The University of Auckland, Private Bag 92019, Auckland 1, New Zealand (o.rohrle@auckland.ac.nz). This work was sponsored by the Department of Energy under grant numbers DE-FC02-01ER25479 and DE-FG02-03ER25574, Lawrence Livermore National Laboratory under contract number B533502, Sandia National Laboratory under contract number 15268, and the National Science Foundation under VIGRE grant number DMS-9810751.

(see (3.2)). We assume that the Oseen equations have a unique solution, which provides the desired  $H^1$  and  $H^2$  regularities (see (3.5) and (3.12)). We are, thus, able to show that  $G_1$  is equivalent to the squared  $L^2$  and  $H^1$  norms and that  $G_2$  is equivalent to the squared product  $H^1$  norm. It should be noted that the constants involved in the equivalences we develop in this paper are naturally dependent on the domain,  $\Omega$ , the Reynolds number,  $\lambda = \frac{1}{\mu}$ , and the approximate velocity,  $\boldsymbol{\beta}$ .

Incompressible Navier-Stokes equations can be approximately solved by initial triangulation of the physical domain using a finite element grid that is as coarse as possible, but fine enough to roughly resolve the domain. A Newton iteration is employed, which involves solving a sequence of Oseen equations, each of which is discretized using a FOSLS formulation. The resulting discrete equations are solved using an algebraic multigrid method (AMG). Once the Navier-Stokes equations on the initial grid are sufficiently resolved, the solution is used as an initial guess for a refined grid. This Nested-Iteration (NI) algorithm is repeated through a sequence of successively finer grids until sufficient resolution of the Navier-Stokes equations is achieved. Numerical results presented in section 6 show that this approach is highly effective. Computation on the finest grid is minimized, which is advantageous because work on the coarse grids is relatively inexpensive. After the first few grids, the solution on one grid is in the basin of attraction of the next finer grid, where only one Newton step, that is, the solution of one Oseen system, is required. The approach here is similar to the NI-Newton-FOSLS-AMG scheme described in [9] and applied to elliptic grid generation in [10].

It is well known that the basin of attraction for such methods can be very small. To get within the basin of attraction, one often has to use on coarser levels more expensive and problem-specific methods such as the Projection Multilevel (PML) method proposed in [11], which treats the nonlinearity of the Navier-Stokes equations directly and does not appeal to any linearization step. This method tends to be more robust and has typically a larger domain of convergence, but is in its current form limited, for example, by its set-up cost and choice of smoother. A more significant advantage of global linearization methods, e.g., the NI-Newton-FOSLS-AMG scheme, is that they rely on the solution of large linear systems of equations and, therefore, can draw upon an extensive repertoire on algorithms and knowledge, in particular, since substantial multigrid research is directed on developing robust, fast, and efficient linear solvers.

In section 2, we provide the first-order system formulation with definitions, notation, and some preliminaries. In section 3, ellipticity and continuity for the functionals are shown. In section 4,  $H^1$  and  $H^2$  regularity is proved under the assumption of uniqueness of the solution of the Oseen equations. The NI-Newton-FOSLS-AMG algorithm is described in section 5. In section 6, numerical results for Kovasznay flow are presented.

## 2. The Oseen equations, its first-order system formulation, and other preliminaries.

Let  $\Omega$  be a bounded, connected domain in  $\mathfrak{R}^n$  ( $n = 2, 3$ ) with Lipschitz continuous ( $C^{0,1}$ ) boundary,  $\partial\Omega$ . Consider the stationary, incompressible Oseen equations with Dirichlet boundary conditions for *velocity*,  $\mathbf{u} = (u_1, \dots, u_n)^t$ , and the usual integral condition for *pressure*,  $p$ , as follows:

$$(2.1) \quad \begin{cases} -\mu\Delta \mathbf{u} + (\nabla \mathbf{u}^t)^t \boldsymbol{\beta} + (\nabla \boldsymbol{\beta}^t)^t \mathbf{u} + \nabla p &= \mathbf{f}, & \text{in } \Omega, \\ \nabla \cdot \mathbf{u} &= g, & \text{in } \Omega, \\ \mathbf{u} &= \mathbf{b}, & \text{on } \partial\Omega, \end{cases}$$

where symbols  $\Delta$ ,  $\nabla$ , and  $\nabla \cdot$  stand for the Laplacian, gradient, and divergence operators, respectively ( $\Delta \mathbf{u}$  is the vector of components  $\Delta u_i$ );  $\boldsymbol{\beta} = (\beta_1, \dots, \beta_n)^t$  is a given  $C^1$  vector function;  $\mu$  is a viscosity constant;  $\mathbf{f}$  is a given vector function;  $g$  is a given scalar function; and  $\mathbf{b}$  is the value of velocity on the boundary. We further assume that

$$\int_{\Omega} p \, d\Omega = 0.$$

For convenience, we adopt the notation introduced in [7]. A new independent variable related to the  $n^2$ -vector function of gradients of the displacement vectors,  $u_i$ ,  $i = 1, \dots, n$ , is introduced below. It is convenient to view the original  $n$ -vector functions as column vectors and the new  $n^2$ -vector functions as either block column vectors or matrices. The velocity variable,  $\mathbf{u} = (u_1, \dots, u_n)^t$ , is a

column vector with scalar components  $u_i$ , so that the gradient,  $\nabla \mathbf{u}^t$ , is a matrix with columns  $\nabla u_i$ . For a function,  $\mathbf{U}$ , with  $n$  vector components  $\mathbf{U}_i$ , we write

$$\begin{aligned}\mathbf{U} &= \nabla \mathbf{u}^t = (\mathbf{U}_1, \mathbf{U}_2, \dots, \mathbf{U}_n) \\ &= (U_{ij})_{n \times n},\end{aligned}$$

which is a matrix with entries  $U_{ij} = \partial u_j / \partial x_i$ ,  $1 \leq i, j \leq n$ . We next define the *trace* operator,  $tr$ , as

$$tr \mathbf{U} = \sum_{i=1}^n U_{ii},$$

the divergence operator,  $\nabla \cdot$ , as

$$(\nabla \cdot \mathbf{U})^t = (\nabla \cdot \mathbf{U}_1, \nabla \cdot \mathbf{U}_2, \dots, \nabla \cdot \mathbf{U}_n)^t,$$

and the curl operator,  $\nabla \times$ , as

$$\nabla \times \mathbf{U} = (\nabla \times \mathbf{U}_1, \dots, \nabla \times \mathbf{U}_n).$$

Note that, in the two-dimensional case,  $n = 2$ , the curl of  $\mathbf{u}$  is naturally defined by means of the scalar function

$$\nabla \times \begin{pmatrix} u_1 \\ u_2 \end{pmatrix} = \partial_1 u_2 - \partial_2 u_1.$$

We also define the tangential operator,  $\mathbf{n} \times$ , componentwise as

$$\mathbf{n} \times \mathbf{U} = (\mathbf{n} \times \mathbf{U}_1, \dots, \mathbf{n} \times \mathbf{U}_n).$$

The inner products and norms on the block column vector functions are defined in the natural componentwise way; for example,

$$\|\mathbf{U}\|^2 = \sum_{i=1}^n \|\mathbf{U}_i\|^2 = \sum_{i,j=1}^n \|U_{ij}\|^2.$$

We use standard notation and definitions for the Sobolev spaces  $H^s(\Omega)^n$ , associated inner products  $\langle \cdot, \cdot \rangle_s$ , respective norms,  $\|\cdot\|_s$ , and semi-norms,  $|\cdot|_s$ , for  $s \geq 0$ . When  $s = 0$ ,  $H^0(\Omega)^n$  is the usual  $L^2(\Omega)^n$ , in which case the norm and inner product are denoted by  $\|\cdot\|$  and  $\langle \cdot, \cdot \rangle$ , respectively.  $L_0^2(\Omega)$  denotes the space of  $L^2(\Omega)$  functions  $p$  such that  $\int_{\Omega} p dx = 0$ . The space  $H_0^s(\Omega)$  is the closure of  $C_0^\infty(\Omega)$ , functions in  $C^\infty(\Omega)$  with compact support in the  $\|\cdot\|_s$  norm. From now on, we omit superscripts,  $n$ , and the domain,  $\Omega$ , if the meaning is clear by context. We use  $H_0^{-1}(\Omega)$  to denote the dual spaces of  $H_0^1(\Omega)$  with norm defined by

$$(2.2) \quad \|\phi\|_{-1,0} := \sup_{\psi \in H_0^1(\Omega)} \frac{\langle \phi, \psi \rangle}{\|\psi\|_1}.$$

We use

$$\|\mathbf{u}\|_\infty := \text{ess sup}_{x \in \Omega} |\mathbf{u}(x)|.$$

Let

$$H(\text{div}; \Omega) := \{\mathbf{v} \in L^2(\Omega)^n : \nabla \cdot \mathbf{v} \in L^2(\Omega)\}$$

and

$$H(\text{curl}; \Omega) := \{\mathbf{v} \in L^2(\Omega)^n : \nabla \times \mathbf{v} \in L^2(\Omega)^{2n-3}\},$$

which are Hilbert spaces under respective norms

$$\|\mathbf{v}\|_{H(\text{div};\Omega)} := (\|\mathbf{v}\|^2 + \|\nabla \cdot \mathbf{v}\|^2)^{\frac{1}{2}}$$

and

$$\|\mathbf{v}\|_{H(\text{curl};\Omega)} := (\|\mathbf{v}\|^2 + \|\nabla \times \mathbf{v}\|^2)^{\frac{1}{2}}.$$

Define their subspaces:

$$H_0(\text{div};\Omega) := \{\mathbf{v} \in L^2(\Omega)^n : \nabla \cdot \mathbf{v} \in L^2(\Omega), \quad \mathbf{n} \cdot \mathbf{v} = 0 \quad \text{on} \quad \partial\Omega\}$$

and

$$H_0(\text{curl};\Omega) := \{\mathbf{v} \in L^2(\Omega)^n : \nabla \times \mathbf{v} \in L^2(\Omega)^{2n-3}, \quad \mathbf{n} \times \mathbf{v} = \mathbf{0} \quad \text{on} \quad \partial\Omega\}.$$

Throughout the paper, we use  $c$  and  $C$  as generic constants whose dependence on problem parameters is specified where they occur. Subscripts are used to denote special constants.

As in [7] for Stokes equations, we introduce the *velocity flux* variable,  $\mathbf{U} = \nabla \mathbf{u}^t$ , and define  $\lambda = \frac{1}{\mu}$ . The incompressible Oseen equations (2.1) may be written as the following equivalent first-order system:

$$(2.3) \quad \left\{ \begin{array}{ll} \mathbf{U} - \nabla \mathbf{u}^t = \mathbf{0}, & \text{in } \Omega, \\ -(\nabla \cdot \mathbf{U})^t + \lambda (\mathbf{U}^t \boldsymbol{\beta} + (\nabla \boldsymbol{\beta}^t)^t \mathbf{u}) + \nabla p = \mathbf{f}, & \text{in } \Omega, \\ \nabla \cdot \mathbf{u} = g, & \text{in } \Omega, \\ \mathbf{u} = \mathbf{b}, & \text{on } \partial\Omega. \end{array} \right.$$

where  $\mathbf{f}$  and  $p$  have been scaled by  $\lambda$ .

Note that the definition of  $\mathbf{U}$ , the continuity condition,  $\nabla \cdot \mathbf{u} = g$  in  $\Omega$ , and the Dirichlet condition  $\mathbf{u} = \mathbf{b}$  on  $\partial\Omega$  imply the respective properties

$$(2.4) \quad \nabla \times \mathbf{U} = \mathbf{0} \quad \text{in } \Omega, \quad \text{tr} \mathbf{U} = g \quad \text{in } \Omega, \quad \text{and} \quad \mathbf{n} \times \mathbf{U} = \mathbf{n} \times \nabla \mathbf{b} \quad \text{on } \partial\Omega.$$

Then, the extended equivalent system for (2.3) is

$$(2.5) \quad \left\{ \begin{array}{ll} \mathbf{U} - \nabla \mathbf{u}^t = \mathbf{0}, & \text{in } \Omega, \\ -(\nabla \cdot \mathbf{U})^t + \lambda (\mathbf{U}^t \boldsymbol{\beta} + (\nabla \boldsymbol{\beta}^t)^t \mathbf{u}) + \nabla p = \mathbf{f}, & \text{in } \Omega, \\ \nabla \cdot \mathbf{u} = g, & \text{in } \Omega, \\ \nabla \times \mathbf{U} = \mathbf{0}, & \text{in } \Omega, \\ \nabla(\text{tr} \mathbf{U}) = \nabla g, & \text{in } \Omega, \\ \mathbf{u} = \mathbf{b}, & \text{on } \partial\Omega, \\ \mathbf{n} \times \mathbf{U} = \mathbf{n} \times \nabla \mathbf{b}, & \text{on } \partial\Omega. \end{array} \right.$$

We close this section by recalling some known results.

LEMMA 2.1.

(1) *There is a constant,  $c_1 > 0$ , dependent only on  $\Omega$ , such that*

$$\|p\| \leq c_1 \|\nabla p\|_{-1,0}, \quad \text{for } p \in L_0^2(\Omega).$$

(2) *There is a constant,  $c_2 > 0$ , dependent only on  $\Omega$ , such that*

$$\|p\| \leq c_2 |p|_1, \quad \text{for } p \in L_0^2(\Omega).$$

*Proof.* For (1) and (2), see Nečas [12] and [13] for a general proof.  $\square$

**THEOREM 2.1.** *Assume that domain  $\Omega$  is a bounded convex polyhedron or has  $C^{1,1}$  boundary. Then, for any vector function,  $\mathbf{v}$ , in either  $H_0(\text{div}; \Omega) \cap H(\mathbf{curl}; \Omega)$  or  $H(\text{div}; \Omega) \cap H_0(\mathbf{curl}; \Omega)$ , there is a constant,  $c_3$ , depending only on  $\Omega$ , such that*

$$(2.6) \quad \|\mathbf{v}\|_1^2 \leq c_3 \left( \|\mathbf{v}\|^2 + \|\nabla \cdot \mathbf{v}\|^2 + \|\nabla \times \mathbf{v}\|^2 \right).$$

*If, in addition, the domain is simply connected, then there is a constant,  $c_4$ , depending only on  $\Omega$ , such that*

$$(2.7) \quad \|\mathbf{v}\|_1^2 \leq c_4 \left( \|\nabla \cdot \mathbf{v}\|^2 + \|\nabla \times \mathbf{v}\|^2 \right).$$

*Proof.* See Theorem 3.7-3.9 in [13] and Lemmas 3.4 and 3.6 in [13].  $\square$

**3. Least-squares functional.** The main objective of this section is to establish ellipticity and continuity of least-squares functionals based on (2.3) and (2.5) in appropriate Sobolev spaces. For simplicity of presentation, in the next two sections, we assume that the boundary conditions are homogeneous, that is, we set  $\mathbf{b} = 0$ .

The two main least-squares functionals considered in this paper are

$$(3.1) \quad G_1(\mathbf{U}, \mathbf{u}, p; \mathbf{f}, g) := \left\| -(\nabla \cdot \mathbf{U})^t + \lambda[\mathbf{U}^t \boldsymbol{\beta} + (\nabla \boldsymbol{\beta}^t)^t \mathbf{u}] + \nabla p - \mathbf{f} \right\|_{-1,0}^2 + \|\nabla \cdot \mathbf{u} - g\|^2 + \|\mathbf{U} - \nabla \mathbf{u}^t\|^2$$

and

$$(3.2) \quad G_2(\mathbf{U}, \mathbf{u}, p; \mathbf{f}, g) := \left\| -(\nabla \cdot \mathbf{U})^t + \lambda[\mathbf{U}^t \boldsymbol{\beta} + (\nabla \boldsymbol{\beta}^t)^t \mathbf{u}] + \nabla p - \mathbf{f} \right\|^2 + \|\nabla \cdot \mathbf{u} - g\|^2 + \|\nabla \times \mathbf{U}\|^2 + \|\nabla \text{tr} \mathbf{U} - \nabla g\|^2 + \|\mathbf{U} - \nabla \mathbf{u}^t\|^2.$$

Define

$$M_1(\mathbf{U}, \mathbf{u}, p) := \|\mathbf{U}\|^2 + \|\mathbf{u}\|_1^2 + \|p\|^2$$

and

$$M_2(\mathbf{U}, \mathbf{u}, p) := \|\mathbf{U}\|_1^2 + \|\mathbf{u}\|_1^2 + \|p\|_1^2.$$

Let

$$\mathbf{V}_0 := \{\mathbf{U} \in H^1(\Omega)^{n^2} : \mathbf{n} \times \mathbf{U} = \mathbf{0} \text{ on } \partial\Omega\},$$

$$\mathcal{V}_1 := L^2(\Omega)^{n^2} \times H_0^1(\Omega)^n \times L_0^2(\Omega),$$

and

$$\mathcal{V}_2 := \mathbf{V}_0 \times H_0^1(\Omega)^n \times (H^1(\Omega)/\mathfrak{R}).$$

The first-order system least-squares variational problem for the incompressible Oseen equations (2.3) is to minimize quadratic functional  $G_i$  over  $\mathcal{V}_i$ ,  $i = 1, 2$ : find  $(\mathbf{U}, \mathbf{u}, p) \in \mathcal{V}_i$  such that

$$(3.3) \quad G_i(\mathbf{U}, \mathbf{u}, p; \mathbf{f}, g) = \inf_{(\mathbf{V}, \mathbf{v}, q) \in \mathcal{V}_i} G_i(\mathbf{V}, \mathbf{v}, q; \mathbf{f}, g).$$

We introduce the following technical result found in [3].

**LEMMA 3.1.** *For any  $u \in L^2(\Omega)$  and  $v \in H^1(\Omega)$ , there exists a constant,  $c_5$ , depending only on  $\Omega$ , such that*

$$(3.4) \quad \|uv\|_{-1,0} \leq c_5 \|u\| \|v\|_1.$$

*Proof.* See Lemma 7 in [3].  $\square$

To establish norm equivalence between  $G_1$  and  $M_1$ , assume that  $\boldsymbol{\beta}$  and  $\lambda$  are such that the Oseen equations (2.1) have a unique solution,  $\mathbf{u} \in H^1(\Omega)^n$  and  $p \in L_0^2(\Omega)$ , for every  $\mathbf{f} \in H_0^{-1}(\Omega)^n$ , where  $\Omega$  has Lipschitz continuous ( $C^{0,1}$ ) boundary. Under this assumption, the following a priori regularity estimate holds: there exists a constant,  $C_{1,r}$ , which depends on  $\lambda$ ,  $\boldsymbol{\beta}$ , and  $\Omega$ , such that

$$(3.5) \quad \|\nabla \mathbf{u}\|^2 + \|p\|^2 \leq C_{1,r} \left( \|\mathbf{f} - \Delta \mathbf{u} + \lambda[(\nabla \mathbf{u}^t)^t \boldsymbol{\beta} + (\nabla \boldsymbol{\beta}^t)^t \mathbf{u}] + \nabla p\|_{-1,0}^2 + \|\nabla \cdot \mathbf{u}\|^2 \right).$$

This result is established in Theorem 4.1.

**THEOREM 3.1.** *Assume that  $\Omega$  has Lipschitz continuous boundary. Then there are two positive constants,  $C_{1,e}$  and  $C_{1,c}$ , depending on  $\lambda$ ,  $\boldsymbol{\beta}$ , and  $\Omega$ , such that, for all  $(\mathbf{U}, \mathbf{u}, p) \in \mathcal{V}_1$ ,*

$$(3.6) \quad C_{1,e} M_1(\mathbf{U}, \mathbf{u}, p) \leq G_1(\mathbf{U}, \mathbf{u}, p; \mathbf{0}, 0) \leq C_{1,c} M_1(\mathbf{U}, \mathbf{u}, p).$$

*Proof.* The upper bound in (3.6) is a simple consequence of the triangle inequality, the Cauchy-Schwarz inequality, and the definition of  $\|\cdot\|_{-1,0}$ . Because of limiting arguments, it is enough to show that the lower bound in (3.6) holds for  $\tilde{\mathcal{V}} = H(\text{div}; \Omega)^n \times H_0^1(\Omega)^n \times L_0^2(\Omega)$ . Now, using (3.5), the triangle inequality, definition (2.2), and equation (3.4), we have

$$(3.7) \quad \begin{aligned} \|\nabla \mathbf{u}\|^2 + \|p\|^2 &\leq C_{1,r} \left( \|\mathbf{f} - \Delta \mathbf{u} + \lambda[(\nabla \mathbf{u}^t)^t \boldsymbol{\beta} + (\nabla \boldsymbol{\beta}^t)^t \mathbf{u}] + \nabla p\|_{-1,0}^2 + \|\nabla \cdot \mathbf{u}\|^2 \right) \\ &\leq 2C_{1,r} \left( \|\mathbf{f} - (\nabla \cdot \mathbf{U})^t + \lambda[\mathbf{U}^t \boldsymbol{\beta} + (\nabla \boldsymbol{\beta}^t)^t \mathbf{u}] + \nabla p\|_{-1,0}^2 + \|\nabla \cdot \mathbf{u}\|^2 \right. \\ &\quad \left. + \|\nabla \cdot (\mathbf{U} - \nabla \mathbf{u}^t)\|_{-1,0}^2 + \lambda^2 \|(\nabla \mathbf{u}^t - \mathbf{U})^t \boldsymbol{\beta}\|_{-1,0}^2 \right) \\ &\leq 2C_{1,r} (G_1(\mathbf{U}, \mathbf{u}, p; \mathbf{0}, 0) + (\lambda^2 c_5^2 \|\boldsymbol{\beta}\|_1^2 + 1) \|\mathbf{U} - \nabla \mathbf{u}^t\|^2) \\ &\leq c_6 G_1(\mathbf{U}, \mathbf{u}, p; \mathbf{0}, 0), \end{aligned}$$

where  $c_6$  depends on  $\lambda$ ,  $\boldsymbol{\beta}$ , and  $\Omega$ .

Since

$$(3.8) \quad \begin{aligned} \langle \mathbf{U}, \mathbf{U} \rangle &= \langle \mathbf{U} - \nabla \mathbf{u}^t, \mathbf{U} \rangle + \langle \nabla \mathbf{u}^t, \mathbf{U} \rangle \\ &\leq \left( \|\mathbf{U} - \nabla \mathbf{u}^t\| \|\mathbf{U}\| + \|\nabla \mathbf{u}^t\| \|\mathbf{U}\| \right), \end{aligned}$$

dividing by  $\|\mathbf{U}\|$  and using (3.7) yields

$$(3.9) \quad \|\mathbf{U}\|^2 \leq c_7 G_1(\mathbf{U}, \mathbf{u}, p; \mathbf{0}, 0),$$

where  $c_7$  depends on  $\lambda$ ,  $\boldsymbol{\beta}$ , and  $\Omega$ . Now combining (3.7) and (3.9) with the Poincaré inequality from Lemma 2.1 yields the lower bound. This completes the proof.  $\square$

The following result can be found in Lemma 3.2 in [7].

**LEMMA 3.2.** *Under the assumptions of Theorem 2.1 with simply connected  $\Omega$ , we have the following:*

(1) *Let  $\boldsymbol{\phi} = (\phi_1, \phi_2)^t$  and  $\mathbf{q} = (q_1, q_2)^t$ ; if each  $q_i \in H_0^1(\Omega) \cap H^2(\Omega)$  and each  $\phi_i \in H^1(\Omega)$  is such that  $\Delta \phi_i \in L^2(\Omega)$  and  $\mathbf{n} \cdot \nabla \phi_i = 0$  on  $\partial\Omega$ , then*

$$(3.10) \quad \alpha |\nabla \cdot \mathbf{q}|_1^2 \leq |\nabla \cdot \mathbf{q} + \text{tr} \nabla \times \boldsymbol{\phi}^t|_1^2 + \|\Delta \boldsymbol{\phi}\|^2,$$

where  $\alpha$  is a positive constant depending only on  $\Omega$ .

(2) Let  $\Phi = (\phi_1, \phi_2, \phi_3)^t$  and  $\mathbf{q} = (q_1, q_2, q_3)^t$ ; if each  $q_i \in H_0^1(\Omega) \cap H^2(\Omega)$  and each  $\phi_i \in H^1(\Omega)^3$  is divergence free with  $\Delta \phi_i \in L^2(\Omega)^3$  and  $\mathbf{n} \times (\nabla \times \phi_i) = \mathbf{0}$  on  $\partial\Omega$ , then

$$(3.11) \quad \alpha |\nabla \cdot \mathbf{q}|_1^2 \leq |\nabla \cdot \mathbf{q} + \text{tr} \nabla \times \Phi|_1^2 + \|\Delta \Phi\|^2,$$

where  $\alpha$  is a positive constant depending only on  $\Omega$ .

To establish norm equivalence between  $G_2$  and  $M_2$ , assume that  $\beta$  and  $\lambda$  are such that the Oseen equations (2.1) have a unique solution,  $\mathbf{u} \in H^2(\Omega)^n$  and  $p \in L_0^2(\Omega) \cap H^1(\Omega)$ , for every  $\mathbf{f} \in L^2(\Omega)^n$  and  $g \in H^1(\Omega)/\mathfrak{R}$ , where  $\Omega$  is either a convex polygon or has  $C^{1,1}$  boundary. Under this assumption, the following regularity holds: there exists a constant,  $C_{2,r}$ , which depends on  $\lambda$ ,  $\beta$ , and  $\Omega$ , such that

$$(3.12) \quad \|\mathbf{u}\|_2^2 + \|p\|_1^2 \leq C_{2,r} \left( \|\Delta \mathbf{u} + \lambda[(\nabla \mathbf{u}^t)^t \beta + (\nabla \beta^t)^t \mathbf{u}] + \nabla p\|^2 + \|\nabla \cdot \mathbf{u}\|_1^2 \right).$$

This result is established in Theorem 4.2.

**THEOREM 3.2.** Assume that  $\Omega$  is either a convex polygon or has  $C^{1,1}$  boundary. Then there are two positive constants,  $C_{2,e}$  and  $C_{2,c}$ , which depend on  $\lambda$ ,  $\beta$ , and  $\Omega$ , such that, for all  $(\mathbf{U}, \mathbf{u}, p) \in \mathcal{V}_2$ ,

$$(3.13) \quad C_{2,e} M_2(\mathbf{U}, \mathbf{u}, p) \leq G_2(\mathbf{U}, \mathbf{u}, p; \mathbf{0}, 0) \leq C_{2,c} M_2(\mathbf{U}, \mathbf{u}, p).$$

*Proof.* The upper bound in (3.13) is straightforward from the triangle and Cauchy-Schwarz inequalities. To prove the lower bound in (3.13), note that the  $H^{-1}$  norm of a function is always bounded by its  $L^2$  norm. Since  $\mathcal{V}_2 \subset \mathcal{V}_1$ , then  $G_1 \leq G_2$  on  $\mathcal{V}_2$ . Hence, by Theorem 3.1, we have

$$(3.14) \quad \|\mathbf{U}\|^2 + \|\mathbf{u}\|_1^2 + \|p\|^2 \leq C_{1,e} G_1(\mathbf{U}, \mathbf{u}, p; \mathbf{0}, 0) \leq C_{1,e} G_2(\mathbf{U}, \mathbf{u}, p; \mathbf{0}, 0).$$

It is, thus, required to show only that

$$\|\mathbf{U}\|_1^2 + \|p\|_1^2 \leq C G_2(\mathbf{U}, \mathbf{u}, p; \mathbf{0}, 0).$$

From Theorem 2.1 and Lemma 2.1, we have

$$(3.15) \quad \|\mathbf{U}\|_1^2 + \|p\|_1^2 \leq C \left( \|\mathbf{U}\|^2 + \|(\nabla \cdot \mathbf{U})^t\|^2 + \|\nabla \times \mathbf{U}\|^2 + \|\nabla p\|^2 \right).$$

Therefore, it suffices to show that

$$(3.16) \quad \begin{aligned} \|(\nabla \cdot \mathbf{U})^t\|^2 + \|\nabla p\|^2 &\leq c_8 \|\mathbf{U}\|^2 + \|\nabla \text{tr} \mathbf{U}\|^2 + \|\nabla \times \mathbf{U}\|^2 \\ &+ \| -(\nabla \cdot \mathbf{U})^t + \lambda(\mathbf{U}^t \beta + (\nabla \beta^t)^t \mathbf{u}) + \nabla p\|^2 + c_9 \|\mathbf{u}\|^2, \end{aligned}$$

for some positive constants  $c_8$  and  $c_9$  to be chosen later. We prove (3.16) only for the case  $n = 3$  because the proof for  $n = 2$  is similar.

First, assume that domain  $\Omega$  is simply connected with connected boundary. Since  $\mathbf{n} \times \mathbf{U} = \mathbf{0}$  on  $\partial\Omega$ , we decompose  $\mathbf{U}$  as

$$(3.17) \quad \mathbf{U} = \nabla \mathbf{q}^t + \nabla \times \Phi,$$

where  $\mathbf{q} \in H_0^1(\Omega)^n \cap H^2(\Omega)^n$  and  $\Phi \in H^1(\Omega)^n$  with  $\nabla \cdot \Phi = \mathbf{0}$  (see [7]). Then, using the inequality  $|x + y|^2 \geq \frac{1}{2}x^2 - y^2$ , the triangle inequality, the Poincaré inequality, (3.11), and regularity (3.12), we have

$$\begin{aligned} c_8 \|\mathbf{U}\|^2 + \|\nabla \text{tr} \mathbf{U}\|^2 + \|\nabla \times \mathbf{U}\|^2 + \| -(\nabla \cdot \mathbf{U})^t + \lambda[\mathbf{U}^t \beta + (\nabla \beta^t)^t \mathbf{u}] + \nabla p\|^2 + c_9 \|\mathbf{u}\|^2 \\ \geq c_8 \|\nabla \mathbf{q}^t\|^2 + c_8 \|\nabla \times \Phi\|^2 + |\nabla \cdot \mathbf{q} + \text{tr} \nabla \times \Phi|_1^2 + \|\Delta \Phi\|^2 \\ + \frac{1}{2} \| -\Delta \mathbf{q} + \lambda[\beta \cdot (\nabla \mathbf{q}^t + \nabla \times \Phi) + (\nabla \beta^t)^t \mathbf{q}] + \nabla p\|^2 \\ - \|\lambda(\nabla \beta^t)^t (\mathbf{u} - \mathbf{q})\|^2 + c_9 \|\mathbf{u}\|^2 \end{aligned}$$

$$\begin{aligned}
&\geq c_8 \|\nabla \mathbf{q}^t\|^2 + c_8 \|\nabla \times \Phi\|^2 + \alpha \|\nabla \cdot \mathbf{q}\|_1^2 + \frac{1}{4} \|\Delta \mathbf{q} + \lambda[(\nabla \mathbf{q}^t)^t \boldsymbol{\beta} + (\nabla \boldsymbol{\beta}^t)^t \mathbf{q}] + \nabla p\|^2 \\
&\quad - \frac{1}{2} \lambda^2 \|\boldsymbol{\beta} \cdot \nabla \times \Phi\|^2 - 2\lambda^2 \|(\nabla \boldsymbol{\beta}^t)^t \mathbf{u}\|^2 - 2\lambda^2 \|(\nabla \boldsymbol{\beta}^t)^t \mathbf{q}\|^2 + c_9 \|\mathbf{u}\|^2 \\
&\geq (c_8 - 2c_2^2 \lambda^2 \|\nabla \boldsymbol{\beta}\|_\infty^2) \|\nabla \mathbf{q}^t\|^2 + (c_8 - \frac{1}{2} \lambda^2 \|\boldsymbol{\beta}\|_\infty^2) \|\nabla \times \Phi\|^2 \\
&\quad + \min\{\alpha, \frac{1}{4}\} \frac{1}{C_{2,r}} (\|\Delta \mathbf{q}\|^2 + \|\nabla p\|^2) + (c_9 - 2\lambda^2 \|\nabla \boldsymbol{\beta}\|_\infty^2) \|\mathbf{u}\|^2 \\
&\geq \min\{\alpha, \frac{1}{4}\} \frac{1}{C_{2,r}} (\|(\nabla \cdot \mathbf{U})^t\|^2 + \|\nabla p\|^2),
\end{aligned}$$

where  $c_2$  is the Poincaré constant;  $\alpha$  is the constant in (3.11); and the last inequality is established by choosing  $c_8$  and  $c_9$  so large that  $c_8 - 2c_2^2 \lambda^2 \|\nabla \boldsymbol{\beta}\|_\infty^2$ ,  $c_8 - \frac{1}{2} \lambda^2 \|\boldsymbol{\beta}\|_\infty^2$ , and  $c_9 - 2\lambda^2 \|\nabla \boldsymbol{\beta}\|_\infty^2$  are positive. This establishes (3.16), which yields the proof of the lower bound in (3.13) for simply connected  $\partial\Omega$ . The proof for convex polygonal domain or a domain whose boundary is  $C^{1,1}$  now follows by an argument similar to the proof of Theorem 3.7 in [13].  $\square$

**4. Regularity estimates.** In this section, we provide  $H^1$  and  $H^2$  regularity estimates of the following Oseen equations in  $\mathfrak{R}^n$ , where  $n = 2, 3$ :

$$(4.1) \quad \begin{cases} -\Delta \mathbf{u} + \lambda[(\nabla \mathbf{u}^t)^t \boldsymbol{\beta} + (\nabla \boldsymbol{\beta}^t)^t \mathbf{u}] + \nabla p &= \mathbf{f}, & \text{in } \Omega, \\ \nabla \cdot \mathbf{u} &= g, & \text{in } \Omega, \\ \mathbf{u} &= \mathbf{0}, & \text{on } \partial\Omega, \end{cases}$$

where  $p \in L_0^2(\Omega)$ ,  $\int_\Omega g \, d\Omega = 0$ , and  $\boldsymbol{\beta}$  is a given  $C^1$  function. We assume that equations (4.1) have a unique solution,  $(\mathbf{u}, p) \in H^1(\Omega)^n \times L_0^2(\Omega)$ , when domain  $\Omega$  is a bounded, connected subset of  $\mathfrak{R}^n$  with Lipschitz continuous boundary  $\partial\Omega$ .

LEMMA 4.1. *Let  $\Omega$  be a domain with Lipschitz continuous boundary. Then, for  $q \in L_0^2(\Omega)$ , there exists a function,  $\mathbf{v} \in H_0^1(\Omega)^n$ , such that*

$$\nabla \cdot \mathbf{v} = q, \quad |\mathbf{v}|_1 \leq c_{10} \|q\|,$$

where  $c_{10}$  is a constant depending only on  $\Omega$ .

*Proof.* See Corollary 2.4 and the proof of Lemma 2.2 in [13] or Lemma 9.2.3 in [14].  $\square$

The next result is the first step toward the  $H^1$  regularity estimate.

LEMMA 4.1. *Assume that  $\Omega$  has Lipschitz continuous boundary. For  $\mathbf{f} \in H_0^{-1}(\Omega)^n$  and  $g \in L_0^2$ , the weak solution of (4.1),  $(\mathbf{u}, p) \in H_0^1(\Omega)^n \times L_0^2(\Omega)$ , satisfies the a priori estimate:*

$$(4.2) \quad \|\nabla \mathbf{u}\| + \|p\| \leq c_{11} (\|\mathbf{f}\|_{-1,0} + \|g\| + \|\mathbf{u}\|),$$

where  $c_{11}$  is a constant that depends on  $\lambda$ ,  $\boldsymbol{\beta}$ , and  $\Omega$ .

*Proof.* Taking the pointwise dot product of the first equation in (4.1) with any  $\mathbf{v} \in H_0^1(\Omega)^n$ , integrating over  $\Omega$ , and using integration by parts yields

$$(4.3) \quad \begin{cases} \langle \nabla \mathbf{u}^t, \nabla \mathbf{v}^t \rangle + \lambda \langle (\nabla \mathbf{u}^t)^t \boldsymbol{\beta} + (\nabla \boldsymbol{\beta}^t)^t \mathbf{u}, \mathbf{v} \rangle - \langle p, \nabla \cdot \mathbf{v} \rangle &= \langle \mathbf{f}, \mathbf{v} \rangle, & \mathbf{v} \in H_0^1(\Omega)^n, \\ \langle \nabla \cdot \mathbf{u}, q \rangle &= \langle g, q \rangle, & q \in L^2(\Omega). \end{cases}$$

Since  $g \in L_0^2(\Omega)$ , we can choose an  $\mathbf{s} \in H_0^1(\Omega)^n$ , according to Lemma 4.1, such that

$$(4.4) \quad \nabla \cdot \mathbf{s} = g \quad \text{and} \quad |\mathbf{s}|_1 \leq c_{10} \|g\|.$$

Then, setting  $\mathbf{w} = \mathbf{u} - \mathbf{s} \in H_0^1(\Omega)^n$  in (4.3), we have, for any  $\mathbf{v} \in H_0^1(\Omega)^n$  and  $q \in L^2(\Omega)$ , that

$$(4.5) \quad \begin{cases} \langle \nabla \mathbf{w}^t, \nabla \mathbf{v}^t \rangle + \lambda \langle (\nabla \mathbf{w}^t)^t \boldsymbol{\beta} + (\nabla \boldsymbol{\beta}^t)^t \mathbf{w}, \mathbf{v} \rangle - \langle p, \nabla \cdot \mathbf{v} \rangle &= \langle \mathbf{f}, \mathbf{v} \rangle - \langle \nabla \mathbf{s}^t, \nabla \mathbf{v}^t \rangle \\ &= \langle \mathbf{f}, \mathbf{v} \rangle - \lambda \langle (\nabla \mathbf{s}^t)^t \boldsymbol{\beta} + (\nabla \boldsymbol{\beta}^t)^t \mathbf{s}, \mathbf{v} \rangle, \\ \langle \nabla \cdot \mathbf{w}, q \rangle &= 0. \end{cases}$$

Taking  $\mathbf{v} = \mathbf{w}$  in the first equation of (4.5) and using the second equation of (4.5), the Poincaré-Friedrichs inequality in Lemma (2.1), and (4.4), we have that

$$(4.6) \quad \begin{aligned} \|\nabla \mathbf{w}^t\|^2 &= \langle \mathbf{f}, \mathbf{w} \rangle - \langle \nabla \mathbf{s}^t, \nabla \mathbf{w}^t \rangle - \lambda \langle (\nabla \mathbf{s}^t)^t \boldsymbol{\beta} + (\nabla \boldsymbol{\beta}^t)^t \mathbf{s}, \mathbf{w} \rangle \\ &\quad - \lambda \langle (\nabla \boldsymbol{\beta}^t)^t \mathbf{w} + (\nabla \mathbf{w}^t)^t \boldsymbol{\beta}, \mathbf{w} \rangle \\ &\leq C \left( \|\mathbf{f}\|_{-1,0} + \|g\| \right) \|\nabla \mathbf{w}^t\| + C \|\nabla \mathbf{w}^t\| \|\mathbf{w}\|, \end{aligned}$$

where  $C$  depends on  $\lambda$ ,  $\boldsymbol{\beta}$ , and  $\Omega$ . Cancelling  $\|\nabla \mathbf{w}^t\|$  on both sides yields

$$(4.7) \quad \|\nabla \mathbf{w}^t\| \leq C (\|\mathbf{f}\|_{-1,0} + \|g\| + \|\mathbf{w}\|).$$

To bound  $p$ , choose a  $\mathbf{v} \in H_0^1(\Omega)^n$  according to Lemma 4.1 such that

$$(4.8) \quad \nabla \cdot \mathbf{v} = p \quad \text{and} \quad |\mathbf{v}|_1 \leq c_{10} \|p\|.$$

Thus, from the first equation of (4.5), using the Poincaré-Friedrichs inequality, and (4.8), we have

$$\begin{aligned} \|p\|^2 &= \langle \nabla \mathbf{w}^t, \nabla \mathbf{v}^t \rangle + \lambda \langle (\nabla \mathbf{w}^t)^t \boldsymbol{\beta} + (\nabla \boldsymbol{\beta}^t)^t \mathbf{w}, \mathbf{v} \rangle - \langle \mathbf{f}, \mathbf{v} \rangle \\ &\quad + \langle \nabla \mathbf{s}^t, \nabla \mathbf{v}^t \rangle + \lambda \langle (\nabla \mathbf{s}^t)^t \boldsymbol{\beta} + (\nabla \boldsymbol{\beta}^t)^t \mathbf{s}, \mathbf{v} \rangle \\ &\leq C (\|\nabla \mathbf{w}^t\| + |\mathbf{s}|_1 + \|\mathbf{f}\|_{-1,0}) |\mathbf{v}|_1 \\ &\leq C (\|\nabla \mathbf{w}^t\| + |\mathbf{s}|_1 + \|\mathbf{f}\|_{-1,0}) \|p\|, \end{aligned}$$

where  $C$  depends on  $\lambda$ ,  $\boldsymbol{\beta}$ , and  $\Omega$ . Cancelling  $\|p\|$  and using (4.7) and (4.4), we have

$$(4.9) \quad \|p\| \leq C (\|\mathbf{f}\|_{-1,0} + \|g\| + \|\mathbf{w}\|).$$

From (4.7),  $\mathbf{w} = \mathbf{u} - \mathbf{s} \in H_0^1(\Omega)^2$ , and (4.4) with the Poincaré-Friedrichs inequality, we have

$$(4.10) \quad \begin{aligned} \|\nabla \mathbf{u}^t\| &\leq \|\nabla \mathbf{w}^t\| + \|\nabla \mathbf{s}^t\| \\ &\leq C (\|\mathbf{f}\|_{-1,0} + \|g\| + \|\mathbf{w}\|), \\ &\leq C (\|\mathbf{f}\|_{-1,0} + \|g\| + \|\mathbf{u}\|), \end{aligned}$$

which, together with (4.9), implies that

$$\|\nabla \mathbf{u}^t\| + \|p\| \leq C (\|\mathbf{f}\|_{-1,0} + \|g\| + \|\mathbf{u}\|).$$

This completes the proof.  $\square$

In the next theorem, we remove the  $\|\mathbf{u}\|$  term in (4.2) by assuming uniqueness of the solution for the Oseen equations.

**THEOREM 4.1.** *Let  $\Omega$  have Lipschitz continuous boundary. Assume that the Oseen equations (4.1) have a unique solution,  $(\mathbf{u}, p) \in H_0^1(\Omega)^n \times L_0^2(\Omega)$ . Then this solution satisfies the following a priori estimate:*

$$(4.11) \quad \|\nabla \mathbf{u}\| + \|p\| \leq c_{11} \left( \|\Delta \mathbf{u} + \lambda[(\nabla \mathbf{u}^t)^t \boldsymbol{\beta} + (\nabla \boldsymbol{\beta}^t)^t \mathbf{u}] + \nabla p\|_{-1,0} + \|\nabla \cdot \mathbf{u}\| \right),$$

where  $c_{11}$  is a constant that depends on  $\lambda$ ,  $\boldsymbol{\beta}$ , and  $\Omega$ .

*Proof.* The proof uses a standard compactness argument. Assume that (4.11) does not hold. Thus, there exists a sequence,  $(\mathbf{u}_i, p_i), i = 1, 2, \dots$ , in  $H_0^1(\Omega)^n \times L_0^2(\Omega)$  such that

$$(4.12) \quad \|\nabla \mathbf{u}_i\| + \|p_i\| = 1, \quad i = 1, 2, \dots,$$

and

$$(4.13) \quad \|\Delta \mathbf{u}_i + \lambda[(\nabla \mathbf{u}_i^t)^t \boldsymbol{\beta} + (\nabla \boldsymbol{\beta}^t)^t \mathbf{u}_i] + \nabla p_i\|_{-1,0} + \|\nabla \cdot \mathbf{u}_i\| \rightarrow 0 \quad \text{as } i \rightarrow \infty.$$

Since  $H_0^1(\Omega)^n$  is compact in  $L^2(\Omega)^n$ , the bounded sequence,  $\mathbf{u}_i \in H_0^1(\Omega)^n$ , has a convergent subsequence, denoted for convenience by  $\mathbf{u}_i$  again, such that

$$(4.14) \quad \lim_{i \rightarrow \infty} \mathbf{u}_i = \mathbf{u} \quad \text{in } L^2(\Omega)^n.$$

Thus, by (4.2), (4.13), and (4.14), we now show that  $(\mathbf{u}_i, p_i)$  is a Cauchy sequence with respect to the  $\|\nabla \mathbf{u}\| + \|p\|$  norm: for given  $\epsilon > 0$ , there exists a positive integer,  $N$ , such that

$$\begin{aligned} & \|\nabla(\mathbf{u}_i - \mathbf{u}_j)\| + \|p_i - p_j\| \\ & \leq C \left( \|\Delta(\mathbf{u}_i - \mathbf{u}_j) + \lambda[(\nabla(\mathbf{u}_i - \mathbf{u}_j)^t)^t \boldsymbol{\beta} + (\nabla \boldsymbol{\beta}^t)^t(\mathbf{u}_i - \mathbf{u}_j)] + \nabla(p_i - p_j)\|_{-1,0} \right. \\ & \quad \left. + \|\nabla \cdot (\mathbf{u}_i - \mathbf{u}_j)\| + \|\mathbf{u}_i - \mathbf{u}_j\| \right) \\ & \leq C \left( \|\Delta \mathbf{u}_i + \lambda[(\nabla \mathbf{u}_i^t)^t \boldsymbol{\beta} + (\nabla \boldsymbol{\beta}^t)^t \mathbf{u}_i] + \nabla p_i\|_{-1,0} + \|\nabla \cdot \mathbf{u}_i\| \right. \\ & \quad \left. + \|\Delta \mathbf{u}_j + \lambda[(\nabla \mathbf{u}_j^t)^t \boldsymbol{\beta} + (\nabla \boldsymbol{\beta}^t)^t \mathbf{u}_j] + \nabla p_j\|_{-1,0} + \|\nabla \cdot \mathbf{u}_j\| + \|\mathbf{u}_i - \mathbf{u}_j\| \right) \\ & \leq \epsilon, \quad \text{for } i, j \geq N. \end{aligned}$$

Let  $(\mathbf{u}, p)$  be a limit of Cauchy sequence  $(\mathbf{u}_i, p_i)$  in the above norm. Then, by the triangle inequality, the definition of  $\|\cdot\|_{-1,0}$ , and (4.13), we have

$$\begin{aligned} & \|\Delta \mathbf{u} + \lambda[(\nabla \mathbf{u}^t)^t \boldsymbol{\beta} + (\nabla \boldsymbol{\beta}^t)^t \mathbf{u}] + \nabla p\|_{-1,0} + \|\nabla \cdot \mathbf{u}\| \\ & \leq \|\Delta(\mathbf{u} - \mathbf{u}_i) + \lambda[(\nabla(\mathbf{u} - \mathbf{u}_i)^t)^t \boldsymbol{\beta} + (\nabla \boldsymbol{\beta}^t)^t(\mathbf{u} - \mathbf{u}_i)] + \nabla(p - p_i)\|_{-1,0} \\ & \quad + \|\nabla \cdot (\mathbf{u} - \mathbf{u}_i)\| + \|\Delta \mathbf{u}_i + \lambda[(\nabla \mathbf{u}_i^t)^t \boldsymbol{\beta} + (\nabla \boldsymbol{\beta}^t)^t \mathbf{u}_i] + \nabla p_i\|_{-1,0} + \|\nabla \cdot \mathbf{u}_i\| \\ & \leq C \left( \|\nabla(\mathbf{u} - \mathbf{u}_i)\| + \|p - p_i\| \right) + \|\Delta \mathbf{u}_i + \lambda[(\nabla \mathbf{u}_i^t)^t \boldsymbol{\beta} + (\nabla \boldsymbol{\beta}^t)^t \mathbf{u}_i] + \nabla p_i\|_{-1,0} \\ & \quad + \|\nabla \cdot \mathbf{u}_i\| \rightarrow 0, \quad \text{as } i \rightarrow \infty. \end{aligned}$$

Therefore, we have

$$\begin{cases} -\Delta \mathbf{u} + \lambda[(\nabla \mathbf{u}^t)^t \boldsymbol{\beta} + (\nabla \boldsymbol{\beta}^t)^t \mathbf{u}] + \nabla p = \mathbf{0}, & \text{in } \Omega, \\ \nabla \cdot \mathbf{u} = 0, & \text{in } \Omega, \\ \mathbf{u} = \mathbf{0}, & \text{on } \partial\Omega. \end{cases}$$

Hence, the assumption of uniqueness of solution of the Oseen equations implies that

$$\mathbf{u} = \mathbf{0} \quad \text{and} \quad p = 0,$$

which is contradiction to (4.12). This completes the proof.  $\square$

Finally, if  $\Omega$  is a convex polygon or has a  $C^{1,1}$  boundary,  $H^2$  regularity can be obtained. For this, we rewrite (4.1) as

$$(4.15) \quad \begin{cases} -\Delta \mathbf{u} + \nabla p = \mathbf{f} - \lambda[(\nabla \mathbf{u}^t)^t \boldsymbol{\beta} - (\nabla \boldsymbol{\beta}^t)^t \mathbf{u}], & \text{in } \Omega, \\ \nabla \cdot \mathbf{u} = g, & \text{in } \Omega, \\ \mathbf{u} = \mathbf{0}, & \text{on } \partial\Omega. \end{cases}$$

**THEOREM 4.2.** *Let  $\Omega$  be a convex polygon or have a  $C^{1,1}$  boundary and assume that (4.1) has a unique solution. Then, for  $\mathbf{f} \in L^2(\Omega)^n$  and  $g \in H^1(\Omega)$ , the solution of (4.1) is in  $H^2(\Omega)^n \times H^1(\Omega)/\mathfrak{R}$  and satisfies*

$$(4.16) \quad \|\mathbf{u}\|_2 + \|p\|_1 \leq C_{2,r} (\|\Delta \mathbf{u} + \lambda[(\nabla \mathbf{u}^t)^t \boldsymbol{\beta} + (\nabla \boldsymbol{\beta}^t)^t \mathbf{u}] + \nabla p\| + \|\nabla \cdot \mathbf{u}\|_1),$$

where  $C_{2,r}$  is a constant dependent on  $\lambda, \boldsymbol{\beta}$  and  $\Omega$ .

*Proof.* Applying well-known regularity results for generalized Stokes (see [13, 15]) to (4.15) and using (4.11) in Theorem 4.1, we have

$$\begin{aligned}
(4.17) \quad \|\mathbf{u}\|_2 + \|p\|_1 &\leq C (\|\mathbf{f} - \lambda[(\nabla \mathbf{u}^t)^t \boldsymbol{\beta} - (\nabla \boldsymbol{\beta}^t)^t \mathbf{u}]\| + \|g\|_1) \\
&\leq C (\|\mathbf{f}\| + \|\nabla \mathbf{u}^t\| + \|g\|_1) \\
&\leq C (\|-\Delta \mathbf{u} + \lambda[(\nabla \mathbf{u}^t)^t \boldsymbol{\beta} + (\nabla \boldsymbol{\beta}^t)^t \mathbf{u}] + \nabla p\| + \|\nabla \cdot \mathbf{u}\|_1).
\end{aligned}$$

□

Note that Theorems 4.1 and 4.2 are used to prove the norm equivalences in Theorems 3.1 and 3.2.

REMARK 4.1. *Substituting  $\mu \mathbf{u}$  for  $\mathbf{u}$ ,  $\mu \mathbf{U}$  for  $\mathbf{U}$ , and  $\mu \boldsymbol{\beta}$  for  $\boldsymbol{\beta}$  throughout sections 3 and 4 yields regularity, coercivity, and continuity in the scaled norms*

$$(4.18) \quad \widehat{M}_1(\mathbf{U}, \mathbf{u}, p) := \mu^2 \|\mathbf{U}\|^2 + \mu^2 \|\mathbf{u}\|_1^2 + \|p\|^2,$$

$$(4.19) \quad \widehat{M}_2(\mathbf{U}, \mathbf{u}, p) := \mu^2 \|\mathbf{U}\|_1^2 + \mu^2 \|\mathbf{u}\|_1^2 + \|p\|_1^2.$$

The first order systems (2.3) and (2.5) more closely resemble the original Oseen equations (2.1) and the functional  $G_2$  in (3.2) now resembles the functional  $G_3$  in (5.5) used in the numerical examples presented in the following sections.

**5. NI-Newton-FOSLS-AMG Algorithm.** In this section, we briefly describe the NI-Newton-FOSLS-AMG algorithm. See [9] for more detail.

Given the steady state, incompressible Navier-Stokes equations,

$$(5.1) \quad \begin{cases} -\mu \Delta \mathbf{u} + (\nabla \mathbf{u}^t)^t \mathbf{u} + \nabla p = \mathbf{0}, & \text{in } \Omega, \\ \nabla \cdot \mathbf{u} = 0, & \text{in } \Omega, \\ \mathbf{u} = \mathbf{b}, & \text{on } \partial\Omega, \end{cases}$$

and an approximate solution,  $(\mathbf{u}_i, p_i)$ , that satisfies the boundary conditions,  $\mathbf{u}_i = \mathbf{b}$  on  $\partial\Omega$ , we replace  $\mathbf{u}$  with  $\mathbf{u} + \mathbf{u}_i$  and  $p$  with  $p + p_i$ , which yields

$$(5.2) \quad \begin{cases} -\mu \Delta \mathbf{u} + (\nabla \mathbf{u}^t)^t \mathbf{u}_i + (\nabla \mathbf{u}_i^t)^t \mathbf{u} + (\nabla \mathbf{u}^t)^t \mathbf{u} + \nabla p = \mathbf{f}_i, & \text{in } \Omega, \\ \nabla \cdot \mathbf{u} = g_i, & \text{in } \Omega, \\ \mathbf{u} = \mathbf{0}, & \text{on } \partial\Omega, \end{cases}$$

where

$$(5.3) \quad \begin{cases} \mathbf{f}_i = \mu \Delta \mathbf{u}_i - (\nabla \mathbf{u}_i^t)^t \mathbf{u}_i - \nabla p_i, & \text{in } \Omega, \\ g_i = -\nabla \cdot \mathbf{u}_i, & \text{in } \Omega. \end{cases}$$

Dropping the nonlinear term,  $(\nabla \mathbf{u}^t)^t \mathbf{u}$ , from (5.2), we arrive at the Oseen equations,

$$(5.4) \quad \begin{cases} -\mu \Delta \mathbf{u} + (\nabla \mathbf{u}^t)^t \mathbf{u}_i + (\nabla \mathbf{u}_i^t)^t \mathbf{u} + \nabla p = \mathbf{f}_i, & \text{in } \Omega, \\ \nabla \cdot \mathbf{u} = g_i, & \text{in } \Omega, \\ \mathbf{u} = \mathbf{0}, & \text{on } \partial\Omega. \end{cases}$$

An approximate solution to (5.4) can be found by minimizing a FOSLS functional over the finite element space for the current grid. For all numerical experiments presented in this paper, we use

$$(5.5) \quad G_3(\mathbf{U}, \mathbf{u}, p; \mathbf{f}_i, g_i) := \|-\mu(\nabla \cdot \mathbf{U})^t + \mathbf{U}^t \mathbf{u}_i + (\mathbf{U}_i^t)^t \mathbf{u} + \nabla p - \mathbf{f}_i\|^2 \\ + \|\nabla \cdot \mathbf{u} - g_i\|^2 + \|2\mu \nabla \times \mathbf{U}\|^2 + \|\mathbf{U} - \nabla \mathbf{u}^t\|^2$$

for this purpose. It follows directly from (5.4) and differs from  $G_2(\mathbf{U}, \mathbf{u}, p; \mathbf{f}, g)$  proposed in (3.2) in the following ways: a rescaling of the momentum equations by  $\mu = 1/\lambda$ ; the missing trace term,  $\nabla \text{tr}(\mathbf{U})$ ; and the scale factor,  $2\mu$ , in the *curl* term. The additional scale factors are used simply

because we observed better numerical performance with them. Concerning the trace term, because of the incompressibility condition expressed by

$$\partial_x u_1 + \partial_y u_2 = U_{11} + U_{22} = 0,$$

we are able to eliminate one of the variables by setting  $U_{11} = -U_{22}$ , which in turn enforces  $\nabla \text{tr}(\mathbf{U}) = \mathbf{0}$  and, therefore, makes this trace equation unnecessary. In three dimensions, a similar procedure can be used to enforce the trace constraint. It should be noted that none of these modifications would change the ellipticity proof of the preceding sections.

Standard linear, quadratic, cubic, and quartic finite elements are used in a Rayleigh-Ritz-type discretization, and a conjugate gradient method preconditioned by algebraic multigrid (AMG) is used for solving the resulting system of equations. Once an acceptable approximation to the solution of (5.4) is computed, the approximate solution of (5.1) is updated as  $\mathbf{u}_{i+1} = \mathbf{u} + \mathbf{u}_i$  and  $p_{i+1} = p + p_i$ . If the new approximation,  $(\mathbf{u}_{i+1}, p_{i+1})$ , is sufficiently close to the best possible approximation on that grid level, the grid is refined and  $(\mathbf{u}_{i+1}, p_{i+1})$  becomes the initial approximation on the refined grid. This is known as a nested iteration (NI) or full multigrid (FMG, c.f. [16, 17]). The approach here is similar to the NI-Newton-FOSLS-AMG scheme described in [9] and applied to elliptic grid generation in [10].

**6. Numerical example.** In this section, we give numerical results on approximating the Navier-Stokes equations by solving a sequence of Oseen equations within the NI-Newton-FOSLS-AMG framework. Our results show optimal finite element approximation properties and efficiency of the nested iteration strategy. Error-versus-work (Figure 6.1) exposes the potential of FOSLS to develop automated and work-optimal solution strategies that are capable of controlling stepsize and polynomial order of finite elements.

All numerical experiments are based on Kovasznay flow, which is named after L.I.G. Kovasznay who derived in [18] an analytic solution for the steady-state, incompressible Navier-Stokes equations for a special laminar flow problem. The problem is posed on a rectangular domain,  $[-.5, 2.0] \times [-.5, 1.5]$ . Knowledge of the exact solution allows us to impose boundary conditions either strongly or weakly. Here, we choose to impose all boundary conditions strongly. Note that for accurate error estimates, FOSLS does not need to appeal to an exact analytic solution, since the FOSLS functional itself naturally provides a sharp error measurement.

Nested iteration aims to improve the overall efficiency of a solution technique by grid continuation. The basic idea behind nested iteration is to provide the solver on successively finer grids with good initial guesses by first solving the problem on coarser levels. The advantage of such a scheme is that it leads to substantially less work on the finer levels by eliminating the need for many iterations there; this is an advantage for linear problems as well. It tends to produce approximations that are in the basin of attraction on all levels. On each level, it remains to be determined when to continue to iterate on the current Newton step, take another Newton step, refine the grid, or stop. A little reflection suggests that the functional itself should be used to make this decision. Since the decrease of the functional must eventually stall on each given level because of discretization error, at some point before that stall it would be inefficient to iterate further and far more productive to refine the grid. To describe this mathematically, let  $G_3(\mathbf{U}_n^l, \mathbf{u}_n^l, p_n^l; \mathbf{f}, g)^{1/2}$  be the functional norm of the current approximation on level  $l$ , and let  $G_3(\mathbf{U}_\infty^l, \mathbf{u}_\infty^l, p_\infty^l; \mathbf{f}, g)^{1/2}$  be an observed estimate of the best that we can do on level  $l$ , meaning that we determine this value by iterating enough on each level to be confident that the functional norm stops changing in the first 4 significant decimal places. We then say that it is more efficient to switch to the next finer level, level  $l + 1$ , if

$$(6.1) \quad G_3(\mathbf{U}_n^l, \mathbf{u}_n^l, p_n^l; \mathbf{f}, g)^{1/2} < (1 + \epsilon) G_3(\mathbf{U}_\infty^l, \mathbf{u}_\infty^l, p_\infty^l; \mathbf{f}, g)^{1/2},$$

for some tolerance  $\epsilon$ . Tolerance  $\epsilon$  reflects what we mean by near the level of discretization error. In this paper, we first compute  $G_3(\mathbf{U}_\infty^l, \mathbf{u}_\infty^l, p_\infty^l; \mathbf{f}, g)$  on all levels. Then, under the objective of finding a cost-optimal strategy, we manually select on each level the smallest amount of Newton steps and multigrid cycles per Newton step that fulfill (6.1) for  $\epsilon = 0.05$ . Of course, first computing  $G_3(\mathbf{U}_\infty^l, \mathbf{u}_\infty^l, p_\infty^l; \mathbf{f}, g)$  on the finest level makes picking an optimal strategy superfluous, but our

objective here is to demonstrate that the Navier-Stokes equations can be solved efficiently in a FOSLS setting. The development of automated nested iteration techniques is the subject of future research. Note that a tolerance of  $\epsilon = 0.05$  is much tighter than what is typically used in most nested iteration or full multigrid processes. A somewhat looser tolerance would likely occur naturally in an automatic NI strategy and lead to fewer Newton steps and V-cycles.

Tables 6.1-6.4 report on numerical experiments for optimal NI strategies to approximate Kovaszny flow with Reynolds number 40 ( $\lambda = 40$ ), using linear (Table 6.1), quadratic (Table 6.2), cubic (Table 6.3), and quartic (Table 6.4) finite elements. In all tables, for each level  $l$ , we report on the minimal number of Newton steps (NS) and V-cycles per Newton step (VC per NS) necessary to satisfy (6.1) with  $\epsilon = 0.05$ , as well as the functional norm,  $G_3^{1/2}$ , resulting from this optimal choice. Additionally, we report on the functional reduction factor as the resolution doubles, defined by

$$(6.2) \quad F^{(l)} = \left( \frac{G_3(\mathbf{U}_n^l, \mathbf{u}_n^l, p_n^l; \mathbf{f}, g)}{G_3(\mathbf{U}_m^{l+1}, \mathbf{u}_m^{l+1}, p_m^{l+1}; \mathbf{f}, g)} \right)^{1/2},$$

where  $G_3(\mathbf{U}_n^l, \mathbf{u}_n^l, p_n^l; \mathbf{f}, g)$  is the functional value on level  $l$  obtained by choosing its level-optimal strategy and  $G_3(\mathbf{U}_m^{l+1}, \mathbf{u}_m^{l+1}, p_m^{l+1}; \mathbf{f}, g)$  the corresponding value on the next finer level. The different subindices,  $n$  and  $m$ , are used to indicate that different numbers of Newton steps and V-cycles per Newton steps can be used on different levels. Independent of the finite element discretization, we start each NI strategy on the same coarse level. This level consists of  $5 \times 4$  square elements (stepsize  $h = 0.5$ ), is denoted by  $l = 0$ , and is used as a guideline for other iteration levels. The next finer level,  $l = 1$ , is constructed by subdividing each element into 4 elements of equal size. Hence, level 1 consists of  $10 \times 8$  elements in all tables. The same refinement strategy is also used on all other levels. So level  $l = 2$  consists of  $20 \times 16$  elements, level  $l = 3$  of  $40 \times 32$  elements, level  $l = 4$  of  $80 \times 64$  elements, and so forth. While in all numerical experiments the number of elements for each level remains the same, the number of grid points (degrees of freedom) varies with the type of finite elements used in the discretization. For example, on level 0, using linear finite elements creates 30 grid points, quadratic finite elements correspond to 99, cubic finite elements result in 208, and quartic finite elements have 357 grid points (with 6 degrees of freedom per grid point). On the coarsest level, we start with a random initial guess. For subsequent linearization steps, we use the current (interpolated) approximation. As the solver, we use conjugate gradients preconditioned by AMG using  $V(1,1)$  cycles and a Gauß-Seidel smoother.

The theory in [10] shows that, under appropriate conditions, our NI-Newton-FOSLS-AMG scheme should converge in one overall step to an approximation on the finest level that is accurate to the level of discretization error. Additionally, the numerical results in [10] suggests that only one Newton iteration is required per level. Tables 6.1-6.4 support these predictions for Kovaszny flow using either linear, quadratic, cubic, or quartic finite elements. On coarser levels, one might need more than one Newton step to get within a specified tolerance of the discretization error. However, on finer levels, one Newton linearization appears to be sufficient to fulfill (6.1). This suggests that the solution on one grid level is close enough to the solution on the next grid level that only one Newton step is required to approximate the solution to the level of discretization error. Moreover, the product  $H^1$  equivalence of our functional is enough to ensure that our AMG method converges uniformly in  $h$  for the linear element case. This optimality is confirmed by the results in Table 6.1. However, performance of standard AMG degrades with higher-order elements and for decreasing  $h$ , which is not surprising because AMG was developed for problems of M-matrix type. To restore optimality, we would need to appeal to improved AMG techniques that are being developed for higher-order finite element matrices (c.f. [19]).

Note that we appear to have obtained optimal finite element approximation properties. On each level, the functional norm stagnates at the level of discretization error. The fact that we reached the level of discretization error is also supported by the functional reduction factors. For smooth enough solutions, standard finite element theory (cf. [14, 8, 13]) establishes an asymptotic functional norm reduction factor for linear finite elements of 2, for quadratic finite elements of 4, for cubic finite elements of 8, and for quartic finite elements of 16 as we double the resolution. The numerically computed functional reduction factors,  $F^{(l)}$ , are reported in column 5 of Tables 6.1-6.4 and coincide

very well with theory. The often slightly lower than theoretical value stems from the fact that our NI strategy moves to a finer grid whenever we are within a certain tolerance of the level of discretization error.

To understand the overall efficiency of our NI scheme, we need to assess its cost. Figure 6.1 illustrates numerical results for the functional norm versus the total work needed to achieve accuracy

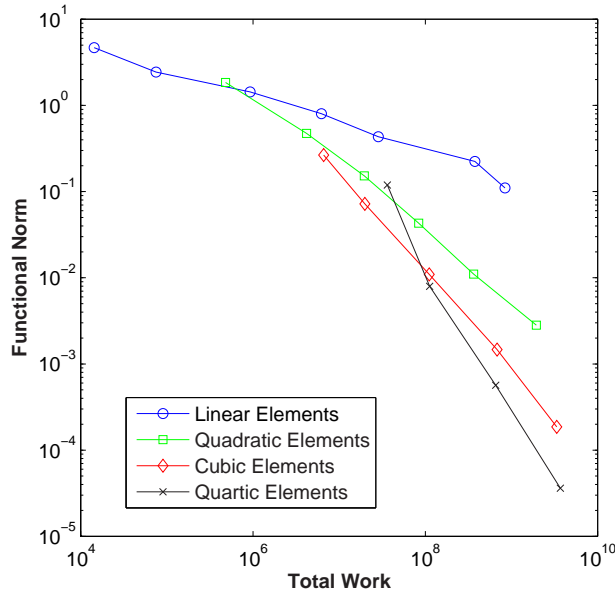


FIG. 6.1. Functional norm versus total work for Kovasznay flow with Reynolds number 40 using different finite element discretizations. The NI strategies presented are based on the results of Tables 6.1-6.4.

to the level of discretization error for different finite element spaces. The total work, TW, is computed by

$$(6.3) \quad TW = \sum_l \left( \sum_\nu \text{complexity}_\nu^l \cdot \text{cycles}_\nu^l \right) \cdot \text{nonzeros}^l,$$

where the summations are over all grid levels,  $l$ , and all Newton steps,  $\nu$ . Here, 'cycles $_\nu^l$ ' is the number of V-cycles done on level  $l$  at Newton step  $\nu$ ; 'nonzeros $^l$ ' is the number of nonzero matrix entries; and 'complexity $_\nu^l$ ' is the cycle complexity, which is computed by summing the number of nonzero matrix entries on level  $l$ , multiplied by the number of relaxation sweeps performed on that level, divided by the number of nonzero entries in the fine-grid matrix.

As a remark on Figure 6.1, note that high accuracy favors high-order finite elements. Better AMG effectiveness for higher-order elements would shift the curves for the higher-order finite element discretizations to the left. It also should be noted that solving Oseen equations without a nested iteration strategy is much more expensive. To demonstrate this, we use the same set-up as in Table 6.1. Now, instead of starting on coarser levels, we start with a random initial guess on the finest level (level  $l = 6$ ). To satisfy (6.1) with the same tolerance,  $\epsilon = 0.05$ , a total of 3 Newton steps and 7 V-cycles per Newton steps are necessary. By (6.3), this approach exceeds the total work for the NI strategy given in Table 6.1 by more than a factor of 2.3.

## REFERENCES

- [1] P.B. BOCHEV AND M. D. GUNZBURGER, *Analysis of least-squares finite element methods for the Stokes equations*, Math. Comp., 63 (1994), pp 479–506.
- [2] P. B. BOCHEV AND M. D. GUNZBURGER, *Least-squares methods for the velocity-pressure-stress formulation of the Stokes equations*, Comput. Methods Appl. Mech. Engrg., 126 (1995), pp 267–287.
- [3] P. B. BOCHEV, T. A. MANTEUFFEL AND S. F. MCCORMICK, *Analysis of velocity-flux least-squares principles for the Navier-Stokes equations. Part I.*, SIAM J. Numer. Anal. 35(1998), pp. 990–1009.
- [4] P. B. BOCHEV, T. A. MANTEUFFEL AND S. F. MCCORMICK, *Analysis of velocity-flux least-squares principles for the Navier-Stokes equations. Part II.*, SIAM J. Numer. Anal. 36(1999), pp. 1125–1144.
- [5] J. H. BRAMBLE, R. D. LAZAROV, AND J. E. PASCIAK, *A least-squares approach based on a discrete minus one inner product for first order system*, Math. comp. 66 (1997), pp 935–955.
- [6] Z. CAI, T. MANTEUFFEL, AND S. MCCORMICK, *First-order system least squares for velocity-vorticity-pressure form of the Stokes equations, with application to linear elasticity*, ETNA, 3 (1995), pp. 150–159.
- [7] Z. CAI, T. MANTEUFFEL, AND S. MCCORMICK, *First-order system least squares for the Stokes equations, with application to linear elasticity*, SIAM J. Numer. Anal., 34 (1997), pp. 1727-1741.
- [8] P. G. CHARLET, *The Finite Element Method for Elliptic Problems*, North-Holland, New York, 1978.
- [9] A. L. CODD, T. A. MANTEUFFEL, AND S. F. MCCORMICK *Multilevel first-order system least squares for non-linear elliptic partial differential equations* SIAM J. Numer. Anal., 41 (2003), pp. 2197–2209 (electronic).
- [10] A. L. CODD, T. A. MANTEUFFEL, S. F. MCCORMICK, AND J. W. RUGE, *Multilevel first-order system least squares for elliptic grid generation*, SIAM J. Numer. Anal., 41 (2003), pp. 2210–2232 (electronic).
- [11] T.A. MANTEUFFEL, S.F. MCCORMICK, O. RÖHRLE, AND J. RUGE, *Projection Multilevel Methods for Quasi-linear Elliptic Partial Differential Equations: Numerical Results*, SIAM J. Numer. Anal., 44 (2006), pp 120–138.
- [12] J. NEČAS, *Sur les normes équivalentes dans  $W_p^k(\Omega)$  et Sur la coercitivité des formes formellement positives, Équations aux Dérivées Partielles*, Les Presses de l'Université de Montréal, Canada, 1965
- [13] V. GIRAULT AND P. A. RAVIART, *Finite Element Methods for Navier-Stokes Equations: Theory and Algorithms*, Springer-Verlag, New York, 1986.
- [14] S. C. BRENNER AND L. RIDGWAY SCOTT, *The mathematical Theory of Finite Element Methods*, Springer-Verlag, 1994.
- [15] R. TEMAMM, *Navier-Stokes Equations, Theory and Numerical Analysis*, North-Holland, Amsterdam, 1985.
- [16] W. L. BRIGGS, V. E. HENSON, AND S. F. MCCORMICK, *A multigrid tutorial*, Society for Industrial and Applied Mathematics (SIAM), 2000
- [17] U. TROTTEMBERG, C. W. OOSTERLEE, AND A. SCHÜLLER *Multigrid* Academic Press Inc.,2001
- [18] L. I. G. KOVASZNY, *Laminar flow behind two-dimensional grid*, Proc. Cambridge Philos. Soc., 44 (1948), pp. 58–62
- [19] J. HEYS, T. A. MANTEUFFEL, S. F. MCCORMICK, AND L. OLSON, *Algebraic multigrid (AMG) for high-order finite elements*, J. Comp. Physics., 195 (2004), pp. 560-575

Level $l$	NS	VC per NS	Functional- norm $G_3^{1/2}$	Factor $F^{(l)}$
0	1	1	4.6821e+00	
1	1	1	2.4416e+00	1.918
2	1	3	1.4372e+00	1.699
3	1	3	8.0246e-01	1.791
4	1	3	4.3277e-01	1.854
5	1	3	2.2375e-01	1.934
6	1	4	1.1024e-01	2.029

TABLE 6.1

*Cost-optimal strategy for Kovaszany flow with Reynolds number 40 using linear finite elements and tolerance  $\epsilon = 0.05$  in (6.1).*

Level $l$	NS	VC per NS	Functional- norm $G_3^{1/2}$	Factor $F^{(l)}$
0	2	2	1.8465e+00	
1	2	3	4.7450e-01	3.891
2	1	5	1.5250e-01	3.111
3	1	5	4.2941e-02	3.551
4	1	6	1.1036e-02	3.891
5	1	9	2.8201e-03	3.940

TABLE 6.2

*Cost-optimal strategy for Kovaszany flow with Reynolds number 40 using quadratic finite elements and tolerance  $\epsilon = 0.05$  in (6.1).*

Level $l$	NS	VC per NS	Functional- norm $G_3^{1/2}$	Factor $F^{(l)}$
0	3	4	2.6549e-01	
1	1	5	7.1924e-02	3.691
2	1	8	1.0957e-02	6.564
3	1	12	1.4664e-03	7.472
4	1	14	1.8621e-04	7.875

TABLE 6.3

*Cost-optimal strategy for Kovaszany flow with Reynolds number 40 using cubic finite elements and tolerance  $\epsilon = 0.05$  in (6.1).*

Level $l$	NS	VC per NS	Functional- norm $G_3^{1/2}$	Factor $F^{(l)}$
0	3	8	1.1947e-01	
1	1	10	7.9668e-03	14.995
2	1	16	5.6538e-04	14.091
3	1	22	3.6122e-05	15.652

TABLE 6.4

*Cost-optimal strategy for Kovaszany flow with Reynolds number 40 using quartic finite elements and tolerance  $\epsilon = 0.05$  in (6.1).*